ELSEVIER

Gait and Posture 15 (2002) 45–55

GAIT & POSTURE

www.elsevier.com/locate/gaitpost

Coordination underlying the control of whole body momentum during sit-to-stand

Darcy S. Reisman [b], John P. Scholz [a,b,*], Gregor Schöner [c]

[a] *Department of Physical Therapy and Interdisciplinary Neuroscience Program, 303 McKinly Laboratory, University of Delaware, Newark, DE 19716, USA*

[b] *Biomechanics and Movement Science Graduate Program, 303 McKinly Laboratory, University of Delaware, Newark, DE 19716, USA*

[c] *Centre de Recherche en Neurosciences Cognitives, CNRS, Marseille, France*

Abstract

The stability of linear and angular momentum of the center of mass (CM) and the underlying coordination of body segments was investigated for a sit-to-stand task to better understand how the nervous system organizes the redundant degrees of freedom available to accomplish this task. From the effector geometry, we derived a mathematical model relating body segment angles and their angular velocities (i.e. state space) to CM angular and linear momentum. We used this model to partition the variability of joint angle and joint velocity configurations into combinations that leave CM momentum invariant and combinations that do not leave CM momentum invariant. The results revealed that subjects used a range of different state-space combinations from trial to trial that were equivalent with respect to producing a stable value of angular and linear momentum. In contrast, body segment combinations that changed the value of momentum were more restricted. Most interesting was the finding that, when standing up under more challenging support surface conditions, the range of state-space combinations used to stabilize momentum was increased. That is, variability increased most strongly for those angle and angular velocity combinations that left CM momentum invariant, with smaller increases registered for combinations that affected CM momentum.

Keywords: Coordination; Sit-to-stand; Nervous system

1. Introduction

Rising from a seated position is a basic functional task that requires coordination of multiple, redundant degrees of freedom (DOFs). Many investigators have attempted to develop an understanding of how the nervous system solves the 'degrees of freedom problem' [1] in motor tasks. Motor redundancy provides a basis for flexible and adaptive behavior, yet how this redundancy is incorporated into the control strategies used by the nervous system is not well understood. A recent investigation of the sit-to-stand task revealed that the redundant DOFs available for this task are organized to limit the variability (across repetitions) of joint angle combinations that change the path of the body's center of mass (CM) while allowing variations in joint angle combinations that stabilize the path of the body's CM [2]. Stability can be defined as the persistence of a particular state in the face of phasic perturbations. Thus, distinctions about the effects of trial-to-trial variability of joint angle combinations (i.e. combinations of DOFs that affect or do not affect CM position) can be viewed as indices of differential stability [3]. This result suggests that motor redundancy is more properly considered an asset that is exploited by the nervous system rather than a problem [4].

What advantage would such a control strategy confer? One proposal is that selectively freeing joint combinations from control that do not change the desired value of variables crucial to task success reduces internal perturbations that occur due to the mechanical coupling among body segments [3,5]. That is, limiting variability of joint angle combinations requires muscle activation that leads, in turn, to reactive forces along the kinematic chain [6]. Those forces must be responded to by additional muscular action to preserve the desired

* Corresponding author. Tel.: +1-302-831-6281; fax: +1-302-831-4234.

E-mail address: jpscholz@udel.edu (J.P. Scholz).

0966-6362/02/$ - see front matter
PII: S0966-6362(01)00158-8

posture or movement pattern of the kinematic chain. Thus, minimizing control action by allowing joint combinations to vary relatively freely if they do not affect the desired values of important task-related variables too severely confers an advantage. This style of CNS control takes advantage of the available motor redundancy. It contrasts with the view that a relatively unique joint configuration is specified to achieve a particular value of important task-related variables [7–9], such as the CM position.

If the CNS actually uses this style of control, then one might expect that performance under extremely challenging task constraints would lead to a selective increase of joint combinations used, i.e. those that are consistent with stable values of important task-related variables. This hypothesis contrasts with the oft stated view that initial performance under challenging or novel task conditions should lead to a reduction in the number of DOFs used to produce the movement [10,11]. Recently, Scholz et al. (in review) reported results that support the former view. When subjects completed the sit-to-stand task on a very narrow base of support with their eyes closed they demonstrated a significant increase in the range of joint combinations used to stabilize the path of the horizontal CM position and, to a lesser extent, the path of the head, when compared to rising from a normal support surface (Scholz et al., in review).

A similar style of control was not evident for control of the vertical path of the CM position, however. Thus, maintaining a stable vertical CM path was not a constraint that led to particular structuring of joint configuration variability. However, more dynamic variables related to vertical CM control that were not studied may be of greater importance. For example, control of CM momentum during sit-to-stand performance has been investigated by researchers because of its potential importance to successful completion of the task [12]. It has been demonstrated that the magnitude and timing of peak horizontal momentum is much less variable across different speeds and age groups than peak vertical momentum [12–14]. This tight regulation of horizontal momentum is thought to be related to postural stability of the task [13,15]. In addition to an upper limit on peak horizontal momentum, it has been demonstrated that there is a minimum amount of linear momentum that is critical in order to achieve an upright position [16]. While these studies on the control of momentum during sit-to-stand demonstrate the importance of momentum for successful achievement of the task, they do not provide insight about the manner in which momentum is controlled.

The purpose of this study was to investigate the stability of linear and angular momentum of the CM and to assess the style of control used to achieve momentum stability. Based on previous research of the sit-to-stand task, we hypothesized that momentum of the CM is an important task variable that is stabilized during sit-to-stand. Further, we hypothesized that variations of the angles and angular velocities of all contributing body segments, across many repetitions, would be selectively coordinated to keep the value of momentum relatively stable. We predicted that this selective use of body segment angles and angular velocities to stabilize momenta would be increased when the task was made more challenging by narrowing the base of foot support, and that the effect would be greatest for control of horizontal momentum.

2. Materials and methods

2.1. Subjects

Six healthy subjects, four female and two male, mean age 27.7 years, participated in this study. Average weight and height of the subjects was 66.82 kg $\pm$ 12.07 and 1.745 m $\pm$ 0.115, respectively. All subjects gave written consent, approved by the Human Subjects Review Committee, before participating in the experiments.

2.2. Equipment and set-up

A VICON (Oxford Metrics, UK) motion measurement and analysis system and two force platforms (Bertec Co., Worthington, OH) were used to collect the experimental data. The system consisted of six infrared video cameras mounted on tripods and arranged in a half sphere on the left side of the subject. Video data was sampled on line at 120 Hz. Measurement error was less than 2 mm for all cameras in the 2.5-m^3 measurement volume.

Spherical markers, 2 cm in diameter and covered with 3M™ brand retro-reflective tape, were applied to the following locations on the left side of the subject's body using self adhesive Velcro and hypo-allergenic adhesive tape: (1) base of the 5th metatarsal; (2) immediately inferior to the lateral malleolus; (3) lateral femoral condyle; (4) greater femoral trochanter; (5) 2 cm inferior to the lateral aspect of the acromion process of the shoulder; (6) the lateral humeral condyle just superior to the radiohumeral junction; (7) styloid process of the radius; (8) directly anterior to the external auditory meatus (EAM); (9) just lateral to the spinous process of the seventh cervical vertebrae; and (10) on the skin over the left pelvis, approximately 20% of the distance from the greater trochanter to the shoulder and one-third of the distance from the posterior to anterior iliac spines (approximately L5/S1 junction) [17].

Two Bertec force plates were placed side by side so that each of the subject's feet was supported by one plate. The force plate signals (Fx, Fy, Fz, Mx, My, Mz) were sampled by an analog-digital converter that was synchronized to the camera system.

2.3. Experimental procedure

Subjects sat on an adjustable, flat piano bench, the height of which was adjusted so that the distance from the top of wooden blocks used to support the feet to the top of the bench seat was 75% of each subject's lower leg length. The knees were placed in 100° of flexion (0° = full extension). The piano bench had crossed legs connecting two support bars, each of which was supported on one of two force plates. One of three different pairs of wooden blocks was used to support the feet, depending on the experimental condition. One of each pair was placed on each of the two force plates in front of the bench. The blocks were secured to the force plates with double-sided tape to prevent rocking during the experiments. Each pair of blocks was 11 cm high and measured either 8, 11 or 35 cm in the anterior-posterior direction. The widest blocks were used for what we refer to as the 'normal' (NO) support condition, in which the entire surface of the foot was supported. We used a wide block in the 'normal' base of support condition rather than the ground to ensure that the distance from the bottom of the feet and the seat were identical in all conditions. The 8- or 11-cm blocks were used in the narrow base (NB) condition for which only the mid-foot of each foot was in support. The 11-cm blocks were used for two subjects who were particularly tall and had very long feet, while the 8-cm blocks were used for the other four subjects. The blocks supported, on average, $35 \pm 3\%$ of a subject's foot length. Subjects performed the experiments barefoot.

In both experimental conditions, the subject was instructed to hold the arms out in front of the shoulders, horizontal to the support surface. The only other instructions subjects were given regarding use of their arms was that they could not throw them above their head or behind their hips. All subjects moved the arms around this initial position to some extent as needed for balance while standing up.

To begin a trial, the subjects were given a verbal 'go' command. The subjects were told that this was not a reaction time task and the verbal signal was just to alert them that they could begin to stand at anytime thereafter. The subjects were told that once they decided to initiate standing up, they should do so as rapidly as possible without falling. Once attaining the upright posture, the subjects were asked to hold that posture until told to sit down by the experimenter (approximately 3 s).

The subject's performance under two experimental conditions was designed to provide varying degrees of task difficulty. Subjects wore a 4.536-kg backpack throughout the experimental session. Their eyes were also closed during each trial of all experimental conditions. In the 'normal' (NO) support condition, subjects obtained normal information from the support surface and the feet were able to apply typical force against the support surface. In the narrow base of support (NB) condition, information from the support surface was drastically reduced and that of the ankle joint was altered because only the mid-foot was supported. Moreover, the foot could not apply typical forces against the support surface to assist with balancing.

2.4. Data reduction

The coordinates of each reflective marker were low-pass filtered in Matlab™ with a 6 Hz cutoff frequency. The force plate signals were down-sampled to 120 Hz to match the kinematics and low-pass filtered at 20 Hz, then scaled to Newtons. Both signals were filtered with a bi-directional 2nd-order, Butterworth digital filter.

The reflective marker coordinates were used to calculate sagittal plane angles between the horizontal and the shank, thigh, pelvis, trunk, cervical spine/head, arm and forearm segments. The location of the total body center of mass at each point in time was calculated using measured body segment lengths [18].

The experimenter used the first upward deviation from baseline of the horizontal and vertical CM acceleration traces to determine movement onset. The end of the upward phase was determined by when the acceleration trace reached zero again after one acceleration followed by one deceleration. The beginning of the plateau of the CM position was used to determine when the subject attained the upright position. The time at which the buttocks lifted off from the seat was determined from the upward motion of the greater trochanter marker with respect to the seat marker. In addition, the initial discontinuous shift of the A-P COP (2) toward the heel marker from its initial position between the seat and feet (due to dual support of the seat and feet) was used to confirm this selection.

After determining the movement period, the portion of the trial from movement onset to termination in the upright position was normalized to 100 in 0.5% steps (200 samples) using a cubic spline interpolation.

Linear momentum of the center of mass was calculated using the following formula:

$$L = mv$$

where m equals the mass of the subject in kilograms and v equals the velocity of the center of mass of the body. Angular momentum about the center of mass was calculated using the following formula:

$$H = \sum (I_i\omega_i + (m_i(d_i \times v_i)x))$$

where m_i is the mass of the ith segment, ω_i is the angular velocity of the ith segment, I_i is the moment of inertia of the ith segment, d_i is the vector from the ith segment CM to the total body CM and v_i is the velocity of the ith segment CM relative to the velocity of the total body CM.

2.5. Dependant variable

2.5.1. Task variable variability

The standard deviation across trials of the horizontal and vertical linear momentum of the CM and the angular momentum about the CM were obtained at each 10% of the movement trajectory as measures of stability of the hypothesized task variables.

2.5.2. State-space variability

'State-space' refers to the combinations of body segment angles (e.g. shank angle), calculated with respect to the horizontal plane, and their angular velocities. The variability of the state-space combinations across trials at each percentage of the movement path was partitioned into two components. The first component of variability is state-space variability that does not change the value of momentum from its mean value across trials. This variability component represents the use of many different body segment angle and angular velocity combinations which all result in the same value of momentum. In other words, to the extent that maintaining a stable value of momentum from trial to trial is important to task success, this first variability component can be considered to reflect task-equivalent solutions to that control, and is referred to in what follows as task-equivalent variability (TEV). In contrast, the second component of variability represents segment angle and angular velocity combinations that lead to different values of momentum on each trial, i.e. represents non-task equivalent solutions (NTEV). These two components of variability are the primary dependent variables of this study. Note that by task-equivalent, we are referring to joint combinations that are equivalent with respect to control of hypothesized task-related variables, or variables that have a special importance to success at the task. These variability components are identical to those referred to in earlier articles by more technical terms, e.g. variance parallel and perpendicular to the UCM, which were specific to technical aspects of the method used to obtain them (see, for example, Appendix A) [2,5].

The partitioning of variability into TEV and NTEV components allows us to identify the extent to which particular styles of control are utilized. For example, the magnitude of each component tells us if all state-space combinations are being controlled equally or if primarily those combinations that move the value of momentum away from its mean are being controlled. Significantly higher TEV compared to NTEV indicates that variability in body segment angle and angular velocity combinations are directed into task-equivalent solutions that keep the value of momentum relatively stable. Relatively low levels of both TEV and NTEV suggests a different style of control, namely, one in which relatively unique state-space combinations were used to achieve a stable value of linear or angular momentum. Alternatively, if both TEV and NTEV were found to be relatively high, this would indicate non-selective control of the state-space by the CNS, i.e. state-space combinations lead to different values of momentum from trial to trial as often as stabilizing a particular momentum value. Finally, relatively high NTEV accompanied by relatively low TEV indicates that state-space combinations are not organized to stabilize a particular value of the hypothesized task-related variable, calling into question the importance of that variable to task success [5].

It is important to point out that the body segment angle and angular velocity combinations that make up TEV and NTEV differ for every value of each momentum variable because a different geometric model relates state-space combinations to the different types of momentum (e.g. angular vs linear; see below). All body segment angle and angular velocity combinations that lead to the same value of whole-body momentum can be represented by a multi-dimensional surface in the state-space of these elements. We have previously referred to such a surface as an uncontrolled manifold (UCM). Each manifold represents, through the geometric model, a given value of a task variable [2,5] (e.g. angular momentum at 5% of the movement).

The mathematical procedure used to estimate TEV and NTEV, the primary dependent measures of this study, involves a linear approximation of the uncontrolled manifold. Actual variation in the body segment angles and angular velocities across trials is then decomposed into a component that lies parallel to this linear subspace (TEV) and a component in its complement (NTEV). Because this method has been described in detail elsewhere [2,5], we provide only a brief account here, in Appendix A.

2.6. Data analysis

The factors in the repeated measures ANOVA for linear and angular momentum were (a) the component of state-space configuration variability (i.e. TEV and NTEV); (b) the condition (NB and NO); and (c) the direction of movement (i.e. horizontal and vertical). A two-way ANOVA (condition by direction) was performed to examine the variability of linear momentum and a one-way ANOVA (condition) was performed to

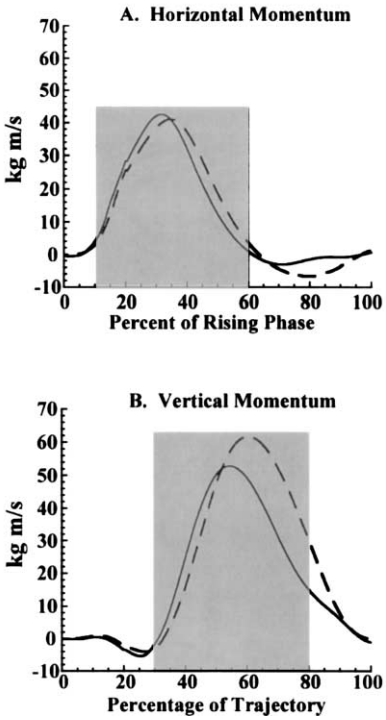

Fig. 1. Mean (across trials and subjects) horizontal (1a) and vertical (1b) linear momentum of the CM for the narrow base (solid line) and normal (dashed line) support surface conditions. The shaded areas indicate the period over which data was averaged.

examine angular momentum variability. When there was a significant effect of a factor or interaction related to our hypotheses, planned contrasts were performed using the SPSS *m*-matrix structure.

The statistical analyses were preformed on averaged data, obtained where the momentum variables demonstrated their greatest change (Figs. 1 and 2). For linear momentum this range was 10–60 and 30–80% of the task period for the horizontal and vertical directions, respectively. For angular momentum this range was 10–60% of the task period. (The data were normalized in time such that lift-off from the seat occurred at 20% of the movement period). However, because the results were relatively consistent throughout the period of greatest change, the averages across these periods were used in the statistical analyses.

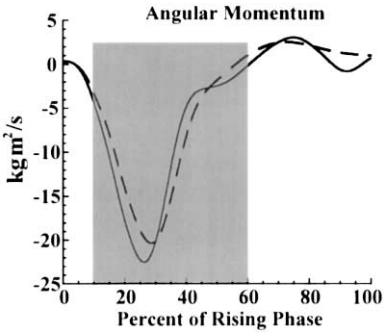

Fig. 2. Mean (across trials and subjects) angular momentum of the CM for the narrow base (solid line) and normal (dashed line) support surface conditions. The shaded area indicates the period over which data was averaged.

3. Results

3.1. Whole-body momentum

3.1.1. Linear momentum of the CM

The mean (across trials and subjects) horizontal and vertical momentum of the CM are presented in Fig. 1. The magnitude of peak horizontal momentum did not differ between the normal (NO) and narrow base (NB) support conditions ($P = 0.312$; Fig. 1a). Peak vertical momentum was larger for the NO condition ($F_{1,5} = 8.494$, $P < 0.05$; Fig. 1b). Overall, peak vertical momentum was higher than peak horizontal momentum, independent of condition ($F_{1,5} = 13.322$, $P < 0.05$).

The time of peak horizontal momentum occured slightly later when standing up on the normal base of support compared to standing up on the narrow base of support ($F_{1,5} = 10.566$, $P < 0.05$). This timing difference between the conditions was even larger for peak vertical momentum ($F_{1,5} = 23.329$, $P < 0.01$).

3.1.2. Angular momentum about the CM

Angular momentum changed similarly across the sit-to-stand movement in both normal (NO) and narrow base (NB) of support conditions (Fig. 2). However, angular momentum was larger (lower minimum) for the NB condition compared to NO ($F_{1,5} = 11.794$, $P < 0.05$). In addition, the minimum of angular momentum occurred significantly earlier in the NB condition ($F_{1,5} = 17.311$, $P < 0.01$).

3.2. Momentum stability

Inter-trial variability (mean across subjects) of the linear momentum of the CM and the angular momentum about the CM are presented in Figs. 3 and 4, respectively, for the entire movement period. Statistical analyses were preformed on the average values for the period of greatest momentum change (see Section 2.6).

3.2.1. Linear momentum stability

There were no significant overall differences in the variability of linear momentum between the NO and NB support conditions ($P = 0.434$), nor were there differences between conditions dependent on the direction of linear momentum ($P = 0.370$). However, horizontal momentum was less variable overall than vertical momentum ($F_{1,5} = 10.978$, $P < 0.05$; Fig. 3). This difference was strongest for the NB condition ($F_{1,5} = 28.91$, $P < 0.01$). The difference between horizontal and verti-

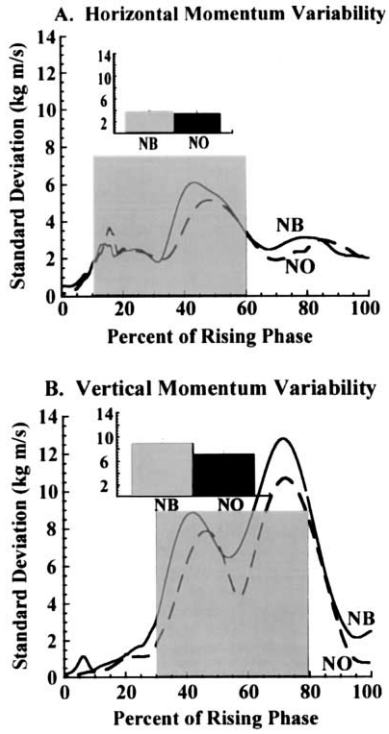

Fig. 3. Mean (across subjects) standard deviation (S.D.) of horizontal (3a) and vertical (3b) linear momentum of the CM for the narrow base (solid line) and normal (dashed line) support surface conditions. Inset bar plot presents the mean S.D. (+SEM) averaged over the period of greatest change of horizontal (10–60%) and vertical (30–80%) (in shaded area), for both conditions (NB = narrow base and NO = normal base of support).

cal momentum variability in the mid-portion of the sit-to-stand movement approached but did not reach significance for the NO condition ($F_{1,5} = 3.78$, $P = 0.11$). Vertical variability was clearly larger than horizontal variability in this condition at the end of the movement period (Fig. 3).

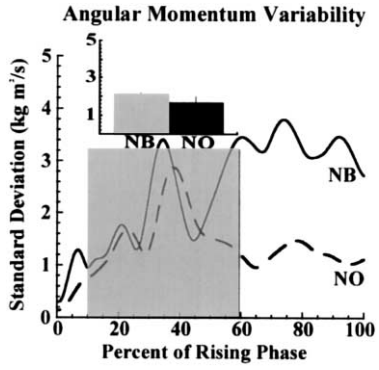

Fig. 4. Mean (across subjects) standard deviation (S.D.) of angular momentum about the CM for the narrow base (solid line) and normal (dashed line) support surface conditions. Inset bar plot presents the mean S.D. (+SEM) averaged over the period of greatest change (10–60%) of angular momentum (in shaded area), for both conditions (NB = narrow base and NO = normal base of support).

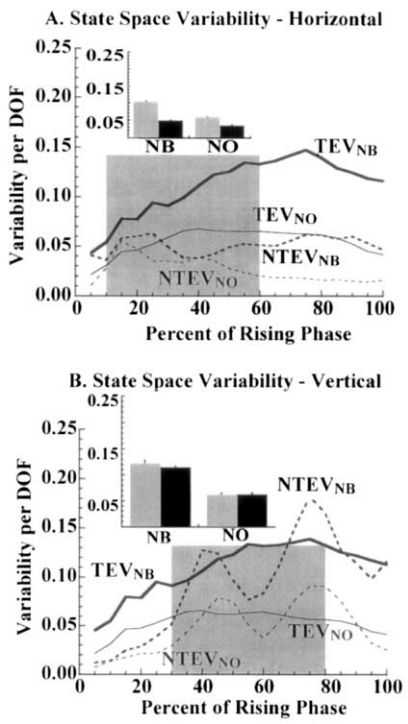

Fig. 5. Mean (across subjects) components of normalized state-space (i.e. body segment angle and angular velocity) variability per degree-of-freedom (DOF) related to controlling horizontal (5a) and vertical (5b) linear momentum of the CM. Solid lines are components of variability consistent with task-equivalent solutions (TEV) to momentum control while dashed lines represent state-space variability leading to a change in momentum from trial to trial (NTEV). Thick lines are results for the narrow base of support condition and thin lines are for the normal base of support condition. Inset bar plot presents the mean state-space variability (+SEM) averaged over the period of greatest change of horizontal (10–60%) and vertical (30–80%) momentum (in shaded area) for both conditions (NB = narrow base and NO = normal base of support). Grey bars: TEV, solid bars: NTEV.

3.2.2. Angular momentum stability

Quantitative differences in angular momentum variability between the experimental conditions did not reach significance ($P = 0.252$) during the period of greatest angular momentum change (e.g. Fig. 2). However, angular momentum variability was larger in NB than in NO during the latter parts of the movement (Fig. 4).

3.3. State-space configuration variability

The results of decomposing the variance of body segment angles and angular velocities into a component (TEV) consistent with a stable momentum value across trials and a component (NTEV) leading to a change in the momentum value from trial to trial are illustrated in Figs. 5 and 6. In those figures, thick lines represent the results for the NB condition, while thin lines represent the results for the NO condition. Solid lines represent the TEV component while dashed lines represent the NTEV component.

3.3.1. Organization of state-space control for stabilizing linear momentum of the CM

Fig. 5a reveals consistent differences between the TEV and NTEV components of state-space variability across the sit-to-stand movement, particularly after lift-off from the seat (i.e. 20%), and consistent differences between the NO and NB conditions, for control of horizontal momentum. State-space variability representing task-equivalent combinations that led to a consistent value of horizontal momentum was significantly higher than NTEV, independent of the condition ($F_{1,5} = 31.97,\ P < 0.01$). TEV was larger in the more challenging NB condition than in the NO condition ($F_{1,5} = 23.5,\ P < 0.01$), while the difference in NTEV between the conditions did not reach significance ($P = 0.103$). Moreover, the difference TEV > NTEV was significantly larger for the NB than the NO condition ($F_{1,5} = 9.53,\ P < 0.05$).

Unlike horizontal momentum, the value of vertical linear momentum was not consistently stabilized across task repetitions (Fig. 5b). In both NB and NO conditions, NTEV displayed a double peak that exceeded TEV at the mid- and late portions of the sit-to-stand movement period. As a result, TEV was not different from NTEV when averaged over the portion of the trajectory representing the greatest change in linear momentum (gray shaded area in Fig. 5b; $P = 0.833$). This lack of a difference between the variance components was similar for both NB and NO conditions ($P = 0.25$), despite larger overall state-space variability for the NB condition ($F_{1,5} = 17.71,\ P < 0.01$; Fig. 5b). Despite the overall similarity in variance components when averaged over the period of greatest vertical momentum change (Fig. 5b), there was a significant difference, TEV > NTEV near the time of peak vertical momentum ($F_{1,5} = 16.82,\ P < 0.05$; cf. Figs 1b and 5b). This was true for both the NB ($F_{1,5} = 10.98,\ P < 0.05$) and NO ($F_{1,5} = 10.37,\ P < 0.05$) conditions.

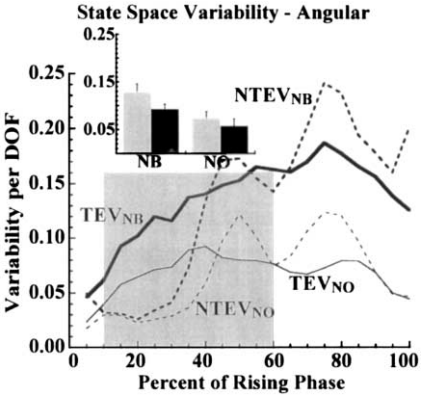

Fig. 6. Mean (across subjects) components of normalized state-space (i.e. body segment angle and angular velocity) variability per degree-of-freedom (DOF) for the control of angular momentum about the CM. Solid lines are components of variability consistent with task-equivalent solutions (TEV) to momentum control while dashed lines represent state-space variability leading to a change in momentum from trial to trial (NTEV). Thick lines are results for the narrow base of support condition and thin lines are for the normal base of support condition. Inset bar plot presents the mean state-space variability (+SEM) averaged over the period of greatest change (10–60%) for angular momentum (in shaded area) for both conditions (NB = narrow base and NO = normal base of support). Grey bars: TEV, solid bars: NTEV.

3.3.2. Organization of state-space control for stabilizing angular momentum about the CM

Differences between the components of state-space variability during the period of greatest angular momentum change (i.e. 10–60%, Fig. 2) depended on the experimental condition (Fig. 6). TEV was significantly higher than NTEV for the NB condition during this period ($F_{1,5} = 7.70,\ P < 0.05$), whereas this difference did not reach significance for the NO condition ($P = 0.15$). As with vertical momentum, however, the difference between TEV and NTEV was significant in the NO condition at the time of peak angular momentum ($F_{1,5} = 21.9,\ P < 0.005$), as was the case with NB ($F_{1,5} = 16.71,\ P < 0.005$).

Both TEV ($F_{1,5} = 19.68,\ P < 0.01$) and NTEV ($F_{1,5} = 9.22,\ P < 0.05$) were significantly higher in the NB condition than in the NO condition. The magnitude of the difference TEV > NTEV was greater for the NB than the NO condition ($F_{1,5} = 14.68,\ P < 0.05$). It is also apparent that overall state-space variability increased and that the differences between TEV and NTEV disappeared or reversed toward the end of the period of greatest angular momentum change, and remained so throughout the remainder of the sit-to-stand movement (Fig. 6). In this sense, angular momentum control was similar to vertical momentum control.

4. Discussion

This study demonstrates the link between task-equivalent solutions to motor coordination and the control of dynamic task-related variables. Combinations of body segment angles and angular velocities were structured selectively to stabilize the values of CM horizontal momentum and, to a lesser extent, angular momentum about the body's CM during performance of a sit-to-stand task. The results of the current analysis indicate that changing the sensory and mechanical conditions to make this well-learned postural task more challenging led to an enhanced use of task-equivalent coordination solutions, i.e. those consistent with a stable value of these task-related variables. Despite the difference in challenge posed by the two experimental conditions, the actual momentum values had similar variability across repetitions, suggesting that this enhanced control strategy in the narrow base condition conferred some advantage.

4.1. Coordination of state-space combinations—stabilization of linear and angular momentum

The structure of state-space control used to stabilize the horizontal momentum of the CM is similar to that previously reported for stabilizing the path of horizontal CM position (Scholz et al., in review). That is, the range of body segment angle and angular velocity combinations consistent with a stable momentum trajectory across task repetitions (i.e. TEV) was significantly larger than the range of combinations leading to a change in whole-body momentum (i.e. NTEV). This finding is not trivial because, theoretically, the use of only one combination of state-space variables from trial to trial could also lead to a consistent momentum trajectory [5]. However, a single combination of state-space variables would require precise control of each joint's trial-to-trial variability, which was not consistent with the current results.

The range of state-space combinations used to stabilize horizontal linear and angular momentum in the current study was larger in the more challenging narrow base of support condition compared to the normal condition. This finding is consistent with our hypothesis that increasing the range of task-equivalent solutions in mechanically unstable task conditions provides an advantage by reducing an additional source of perturbation that would normally occur due to the mechanical coupling of joints [19]. It is also consistent with the observed joint control structure for stabilizing CM and head position reported earlier (Scholz et al., in review). Thus, it appears that a general feature of joint coordination for more difficult postural tasks is to selectively increase the range of state-space combinations, i.e. freeing of directions in state-space which are consistent with the stability of important task variables such as CM position and momentum.

The advantage of greater TEV component variability in the NB condition compared to the NO condition is also apparent from the results on momentum variability (Figs. 3 and 4). Despite the substantial challenge posed by standing up as fast as possible on a narrow base of support without vision, momentum variability did not differ from that for the normal support condition. In contrast, state-space variability increased differentially, with more variability directed into task-equivalent solutions in the NB than in the NO condition. The enhanced variability in state-space was thus structured such that the overall task variable variability remained unchanged. In order for variability to be larger in directions of state-space along which task variables remain invariant than in directions along which task-related variables change, individual joint angles and velocities must be coordinated. More pronounced differences between the two components of variability under more challenging task conditions thus reflect INCREASED coordination.

The results for angular momentum control were not as dramatic as for horizontal momentum control, although a similar style of control was shown during the period of greatest angular momentum change (i.e. during the early portions of the sit-to-stand movement), including similar differences between the experimental conditions. However, the variability structure (TEV > NTEV) was lost after about 40% of the movement period. Thereafter, overall state-space variability related to angular momentum control increased non-selectively. This suggests that control of angular momentum is essential only up to the time of its peak (about 30% of the movement; Fig. 2).

4.2. Differences in the stability of horizontal and vertical momentum

Performance stability, as used here, refers to persistence of system states in the face of phasic perturbations. Such stability, in a control-theoretic sense, can be assessed by examining the structure of variability that occurs with performance under identical experimental conditions across trials.

Many studies have reported that the timing and magnitude of peak horizontal momentum are more consistent than for vertical momentum across different speeds of rising and across ages [12–15]. While these results demonstrate a constancy of horizontal momentum in comparison to vertical momentum, this constancy differs greatly from our definition of stability. We examined the *variability* of momenta across multiple repetitions of the task, for a given task condition, as an index of stability [3]. In contrast, most reports citing differences between horizontal and vertical momentum refer to the consistency in their mean peak values across experimental conditions (e.g. different speeds) or types of subject [12,13,15]. This is comparable to our data demonstrating that there are no significant differences in the mean value of the momentum peak between conditions in the horizontal direction, while there are differences between the narrow base and normal conditions in the vertical direction (Fig. 1). Such analyses do not adequately address the question of stability of performance within a condition for a given subject, which we emphasize in this report.

It has previously been argued that control of a variable by the nervous system results in stable properties of that variable [3]. In view of this definition of stability, our results indicate that horizontal momentum appears to be more tightly regulated than vertical momentum in both the narrow and normal base of support conditions. It has been shown that the additional mechanical constraint provided by a narrow base of support limits the range of available horizontal momen-

tum values if postural stability in the upright position is to be achieved [20]. This limitation in range appears to affect not only the peak magnitude of horizontal momentum (which was significantly lower than peak vertical momentum), but also the stability of momentum production. Thus, the mechanical constraint of a narrow base of support has an unequal effect on horizontal and vertical momentum magnitudes and momentum stability.

4.3. Differences in state-space coordination underlying horizontal and vertical linear momentum control

The greater stability (i.e. lower variability) of horizontal momentum compared to vertical momentum values was reflected in differences in state-space coordination. Throughout most of the sit-to-stand movement, subjects displayed a relatively large range of angle and angular velocity combinations that were *inconsistent* with a stable value of vertical momentum (i.e. NTEV). This range of NTEV was actually enhanced when standing up on the narrow base of support. Thus, the structure of state-space variability underlying the control of vertical momentum was consistent with a stable value of vertical momentum only around the time of peak vertical momentum (60% of trajectory, Fig. 6).

In contrast to vertical momentum, the control of horizontal CM momentum was marked by the use of a large range of task-equivalent solutions (i.e. TEV) that stabilized the value of horizontal momentum across multiple repetitions, while NTEV was restricted. Moreover, this style of coordination (i.e. TEV > NTEV) was enhanced when performing under more challenging task conditions (Fig. 5a). A similar structure of joint coordination has also been reported for control of the path of horizontal CM positions (Scholz et al., in press). This finding contrasts to a previous suggestion that control of the momentum of the CM may be more important than control of its position [20]. Both appear to be equally important.

4.4. Conclusion

It is commonly assumed that the redundancy of the motor system presents a control 'problem' for the CNS when producing functional motor acts [1]. One solution to this 'problem' that is often proposed is to bring to bear additional constraints, often in the form of cost functions, which limit the allowable coordination solutions to only one or a few [8,9,21] (but see Cruse et al. [7]). Although additional task constraints probably determine which solutions are actually realized to some extent, the results of this study and those of earlier work [2,5] (Scholz et al., in review) suggest that a general mode of CNS operation involves the instantiation of a control law in which task-equivalent solutions to the coordination of the motor elements (e.g. joints) are freed to an extent from control, the exact solution depending on momentary changes in internal dynamics and task constraints. Coordination solutions that lead to a change in the value of important task-related variables are constrained. In this way, motor redundancy becomes part of the solution rather than a 'problem'.

This study also revealed the important finding that when the task was made more difficult, the structure of state space fluctuations was accentuated, variability in directions of state space that did not affect the CM horizontal momentum increasing more than variability affecting CM horizontal momentum. For this to occur, the degree of coordination among the movement components must be increased.

Finally, the results of this and earlier work (Scholz et al., in review) suggest that consistent control of both horizontal CM position and its momentum are of greater importance to successful sit-to-stand performance than the control of vertical CM position and momentum. Stabilizing a particular value of vertical momentum appears to be important only near the time of the momentum peak.

Acknowledgements

This work was supported by grant HD35857 from the National Institutes of Health, Child Health and Human Development awarded to Dr Scholz. The authors wish to thank the reviewers for their helpful suggestions. The authors are grateful to Dr Horak and two anonymous reviewers for their many helpful suggestions for revision of the original manuscript.

Appendix A. Procedure to estimate TEV and NTEV

The initial step in estimating TEV and NTEV is to obtain the geometric model relating the task variable, r, (e.g. the horizontal, y, and vertical, z, linear momentum of the CM) to the state-space configuration, θ and ω. In our experiment, the state-space configuration for the hypothesis about controlling the linear momentum of the CM is composed of eight angles (foot, shank, thigh, pelvis, trunk, head/neck, arm and forearm segment angles with the horizontal) and their respective instantaneous velocities. Small changes in r are related to changes in θ and ω through the Jacobian, which is the matrix of partial derivatives of the task variable, r, with respect to the body segment angles and angular velocities, θ and ω. For example, if the task variable under consideration is the horizontal linear momentum of the CM, the geometric

model relating horizontal linear momentum of the CM and the state-space configuration is

$$\mathrm{LM}_{\mathrm{CM}y} = \mathrm{LM}_{\mathrm{FOOT}y} + \mathrm{LM}_{\mathrm{SHANK}y} + \mathrm{LM}_{\mathrm{THIGH}y} + \cdots + \mathrm{LM}_{\mathrm{C\text{-}SPINE}y}$$

where, for example,

$$\mathrm{LM}_{\text{shank-}y} = m_{\mathrm{shank}}\dot{\mathrm{CM}}_{\mathrm{shank}}$$

and

$$\mathrm{CM}_{\mathrm{shank}} = y_{\mathrm{toe}} + l_{\mathrm{foot}}\cos(\theta_{\mathrm{foot}}) + m_{\mathrm{shank}}r_{\mathrm{shank}}\cos(\theta_{\mathrm{shank}}).$$

The mass of the segment is m_i, r_i is the distance of the CM of the segment from the distal end, and θ_i is the angle of the segment with the horizontal. The geometric model relating angular momentum about the CM to the state-space configuration is:

$$(I_{\mathrm{foot}}\omega_{\mathrm{foot}} + m_{\mathrm{foot}}(d_{\mathrm{foot}} \times v_{\mathrm{foot}})_x) + (I_{\mathrm{shank}}\omega_{\mathrm{shank}} + m_{\mathrm{shank}}(d_{\mathrm{shank}} \times v_{\mathrm{shank}})_x) + \cdots + (I_{\mathrm{forearm}}\omega_{\mathrm{forearm}} + m_{\mathrm{forearm}}(d_{\mathrm{forearm}}v_{\mathrm{forearm}})_x).$$

Each term can be expanded to:

$$I_i\omega_i + m_i(d_{yi\,x}v_{zi})_x - m_i(d_{zi}\,v_{yi})_x,$$

where

$$d_{yi} = \mathrm{CM}_{yi} - \mathrm{CM}_y, \quad d_{zi} = \mathrm{CM}_{zi} - \mathrm{CM}_z$$

$$v_{yi} = \dot{\mathrm{CM}}_{yi} - \dot{\mathrm{CM}}_y = \left(\dot{y}_{i-1} - r_i \sin\theta_i\omega_i\right) - \dot{\mathrm{CM}}_y$$

$$v_{zi} = \dot{\mathrm{CM}}_{zi} - \dot{\mathrm{CM}}_z = \left(\dot{z}_{i-1} - r_i \sin\theta_i\omega_i\right) - \dot{\mathrm{CM}}_z$$

where y_{i-1} and z_{i-1} = the segment distal to segment i, r_i = the distance from CM of segment i to the distal end of segment i, θ_i = the segment angle with the horizontal, ω_i = the angular velocity of segment i and CM_{yi}, CM_{zi} are the horizontal and vertical position of the CM of segment i, respectively. The terms CM_y, CM_z, coordinates of the CM of the body, and y_{i-1}, z_{i-1}, coordinates of the joint center distal to the current segment i, are also expressed in terms of the full geometric model (i.e. in terms of segment lengths and angles). The model for angular and linear momentum and their partial derivatives with respect to each body segment angle and angular velocity (i.e. for the Jacobian) were developed step by step using Maple.

The second step is to estimate the linear approximation to the UCM from the geometrical model. Because the UCM differs for each value of the task variable, a decision is necessary as to what value to use for the estimation. In reality, both state-space configurations and task variables vary from trial to trial. Based on the assumption that the normalization of movement time has aligned matching states of the underlying (theta, omega) state space across trials, we computed the mean state-space configuration, $\bar{\theta}$ and $\bar{\omega}$ at each percent of the movement. Effectively, the value of the task variable, $\bar{y}_{\mathrm{CM}}$, associated with that mean state-space configuration was used to construct the UCM. The linear approximation to the UCM was obtained from the geometrical model, linearized around the mean state-space configuration:

$$y_{\mathrm{CM}} - \bar{y}_{\mathrm{CM}} = \underline{\underline{J}}(\bar{\theta}, \bar{\omega}) * \begin{pmatrix} \underline{\theta} - & \bar{\theta} \\ \underline{\omega} - & \bar{\omega} \end{pmatrix}$$

Here, $\underline{\underline{J}}$ is the Jacobian, composed of $\partial y/\partial\theta_i$ and $\partial y/\partial\omega_i$, where $i = \{\text{foot, shank, thigh, pelvis, trunk, head/neck, arm, forearm}\}$. The linear approximation of the UCM is then the null-space of the Jacobian (the linear subspace of all deviations from the mean state-space configuration that are mapped onto zero by the Jacobian). Using Matlab™ for the numerical computation of the null-space, the actual value of the state-space configuration minus the mean state-space configuration at each point along the movement path of each trial is decomposed into a component that lies within this null space and a component in its complement.

Actually, because the state space is composed of variables having different dimensions, i.e. angles in radians and angular velocities in radians per second, a scaling of the Jacobian was necessary before estimating the null space to render the dimensions of the space commensurate. A corresponding scaling of the mean-free state-space vector of each trial was then performed before its projection onto the null space to determine the variability components. The following relationship was used as a basis for this scaling. Harmonic motion involves the following relationship between position and velocity variables:

$$\mathrm{scale}\left(\dot{\theta}\right) = (2\pi/T) * \mathrm{scale}(\theta),$$

where T is the movement period, or twice the movement time. Thus, the scaling was accomplished by multiplying the velocity components of the state-space vector by (MT/π) and by multiplying the appropriate velocity terms of the Jacobian matrix (e.g. $\partial\mathrm{LM}/\partial\omega_i$) by (π/MT) so that all dimensions had units of radians.

The variance (across trials) of the projected components of each trial's harmonically scaled state space vector was then calculated for each experimental condition and normalized by the number of degrees of freedom. For example, for the hypothesis about controlling horizontal linear momentum of the CM, the state-space configuration is 16-dimensional and the task variable is 1-dimensional. Therefore, the null space has fifteen dimensions. Thus, variance of the state-space configuration that lies parallel to the

UCM (i.e. TEV) is divided by 15. The variance perpendicular to the UCM (i.e. variability that changes the value of the task variable from its mean value, NTEV) is divided by one. The square root of this normalized variance was obtained for the data analyses, which is reported as variability per degree of freedom.

References

[1] Bernstein NA. The Coordination and Regulation of Movements. London: Pergamon Press, 1967.

[2] Scholz JP, Schöner G. The uncontrolled manifold concept: identifying control variables for a functional task. Exp Brain Res 1999;126:289–306.

[3] Schöner G. Recent developments and problems in human movement science and their conceptual implications. Ecol Psychol 1995;8:291–314.

[4] Gelfand IM, Latash ML. On the problem of adequate language in motor control. Mot Control 1998;2:306–13.

[5] Scholz JP, Schöner G, Latash M. Identifying the control structure of multijoint coordination during pistol shooting. Exp Brain Res 2000;135:382–404.

[6] Flash T, Hogan N. The coordination of arm movements: an experimentally confirmed mathematical model. J Neurosci 1985;5:1688–703.

[7] Cruse H, Brüwer M, Dean J. Control of three- and four-joint arm movement: strategies for a manipulator with redundant degrees of freedom. J Mot Behav 1993;25:131–9.

[8] Rosenbaum DA, Meulenbroek RG, Vaughan J, Jansen C. Coordination of reaching and grasping by capitalizing on obstacle avoidance and other constraints. Exp Brain Res 1999;128:92–100.

[9] Seif-Naraghi AH, Winters JM. Optimized strategies for scaling goal-directed dynamic limb movements. In: Winters JM, Woo SL-Y, editors. Multiple Muscle Systems. Biomechanics and Movement Organization. New York: Springer-Verlag, 1990:312–34.

[10] Vereijken B, van Emmerik REA, Whiting HTA, Newell KM. Free(z)ing degrees of freedom in skill acquisition. J Mot Behav 1992;24:133–42.

[11] McDonald PV, van Emmerik REA, Newell KM. The effects of a practice on limb kinematics in a throwing task. J Mot Behav 1989;21:245–64.

[12] Pai YC, Rogers MW. Control of body mass transfer as a function of speed of ascent in sit-to-stand. Med Sci Sports Exerc 1990;22:378–84.

[13] Pai YC, Naughton BJ, Chang RW, Rogers MW. Control of body centre of mass momentum during sit-to-stand among young and elderly adults. Gait Posture 1994;2:109–16.

[14] Riley PO, Schenkman ML, Mann RW, Hodge WA. Mechanics of a constrained chair rise. J Biomech 1991;24:77–85.

[15] Pai YC, Lee WA. Effect of a terminal constraint on control of balance during sit-to-stand. J Mot Behav 1994;26:247–56.

[16] Riley PO, Krebs DE, Popat RA. Biomechanical analysis of failed sit-to-stand. IEEE Trans Rehabil Eng 1997;5:353–9.

[17] de Looze MP, Kingma I, Bussman JBJ, Toussaint HB. Validation of a dynamic linked segment model to calculate joint moments in lifting. Clin Biomech 1992;7:161–9.

[18] Winter DA. Biomechanics and Motor Control of Human Movement. New York: John Wiley & Sons, 1990.

[19] Hollerbach MJ, Flash T. Dynamic interactions between limb segments during planar arm movement. Biol Cybern 1982;44:67–77.

[20] Pai YC, Patton J. Center of mass velocity-position predictions for balance control. J Biomech 1997;30:347–54.

[21] Horak F, Kuo A. Postural adaptation for altered environments, tasks, and intentions. In: Winters JM, Crago P, editors. Biomechanics and Neural Control of Posture & Movement. New York: Springer-Verlag, 2000:267–81.